WETTABILITY CHARACTERISTICS VARIATION OF NYLON 6,6 BY MEANS OF CO_2 LASER GENERATED SURFACE PATTERNS

Paper (P116)

D. G. Waugh and J. Lawrence

Wolfson School of Mechanical and Manufacturing Engineering, Loughborough University, Leicestershire, LE11 3TU, UK

Abstract

CO_2 lasers can be seen to lend themselves to materials processing applications. These types of lasers have been used extensively in research and industry with the work carried out being well documented. This work investigated the surface modification of nylon 6,6 with a CO_2 laser in order to vary wettability characteristics. The wettability characteristics of the nylon 6,6 were modified by generating a number of patterns of various topography on the surface using the CO_2 laser. Thereafter the as-received and modified surfaces were analysed using white light interferometry to quantify the topographical changes. Any changes in the chemical composition of the surfaces were explored with EDX and XPS analysis. To quantify the wettability characteristics as a function of laser irradiation, contact angles where determined using a sessile drop device for each sample. In this way it was possible to determine the efficacy of the CO_2 laser generated topographical patterns in terms of wettability characteristics modification. It has been proposed that the increase in contact angle for the laser irradiated samples is due to a change in wetting regime from Wenzel to Cassie-Baxter.

Introduction

On account of its bulk properties nylon can be utilized within the biomaterial industry [1] as sutures [2], vascular grafts and other hard tissue implants [3]. However, from this previous work it is widely accepted that the polymer surface does not give rise to adequate cell adhesion and proliferation. Due to the shortfall in polymer surface characteristics, with regards to bioactivity, one can see that it may be an advantage to implement a method whereby the bioactivity of the nylon is increased. Numerous techniques have been employed to produce surface variations in the form of topography and surface chemistry modifications: radiation grafting [4], plasma surface modification [5,6] and using various coatings [7]. Laser surface modification is another method which can be implemented for such biological applications [8-10] and offers a number of benefits, such as relative cleanliness, accuracy and non-contact processing.

Previous and current research has identified that it is crucial that any biomaterial should be optimized such that they can function appropriately and efficiently within the desired biological environment [11]. In many applications it is seen that the bulk properties of a biomaterial are decided upon such that the surface properties are compromised [12,13]. This is evident in the case of polymeric biomaterials. Although they offer bulk properties which are ideal for biological applications, they possess surface properties that do not lend themselves to high performance with regards to cell adhesion and proliferation [14]. To counteract this, it would be ideal to modify the surface properties of the material without hindering the bulk properties in order to influence wettability and bioactivity.

It has also been found that the wettability characteristics of a material has a direct link to the bioactivity [1,15,16]; however, no complete mathematical theory has been derived as the mechanisms involved appear to be many and complex. Through the available literature it can be seen that extensive research is now being carried out regarding this in the endeavour to link wettability and bioactivity of materials [17,18].

The CO_2 laser is one of the most used lasers throughout the scientific world and within many industries due to it being one of the most versatile. This laser family has the ability of emitting radiation within the infra-red (IR) region of the electromagnetic spectrum on rotational-vibrational transitions with wavelengths ranging from 9 to 11μm [19]. On the account of the CO_2 lasers versatility and high powers they have been implemented for many years in the general field of materials processing from cutting to alloying.

In this paper a CO_2 laser system has been employed to produce various patterns on the surface of a

biopolymer, nylon 6,6. Since wettability characteristics have been shown to be a driver for enhancing the bioactivity of a material in terms of cell adhesion and proliferation [13]. These surface patterns have been analysed to determine the effect they have on the wettability characteristics of the polymer.

Experimental Technique

Material

The nylon 6,6 was sourced in 100mm×100mm sheets with a thickness of 5mm (Goodfellow Cambridge, Ltd). To obtain a conveniently sized sample for experimentation, the as-received nylon sheet was cut into 30mm diameter discs using a 1kW cw CO_2 laser (Everlase S48; Coherent Ltd). Under optical microscopic examination there was no discernible heat affected zone (HAZ).

CO_2 Laser Irradiation Procedure

The 10.6μm wavelength Synrad cw 10W CO_2 laser system, with a spot size of the order of 70μm, is housed at Loughborough University and uses a galvanometer scanner to scan the beam directly across the target material. The nylon 6,6 target material and laser system were held in a laser safety cabinet in which the ambient gas was air. An extraction system was used to remove any fumes produced during the laser processing. In order to generate the required marking pattern the Synrad Winmark software version 2.1.0, build 3468 was used. In addition, the software was capable of using images saved as .dxf files which can be produced by using CAD programs such as, in this case, Licom AutoCaM.

The nylon 6,6 samples were irradiated using the CO_2 laser system generating a number of surface patterns: spiral (diameter 30mm with 50μm spacing), concentric circles (50μm spacing between the circumference of each circle), triangular (a square 2000μm×2000μm with opposite corners joined to produce 4 triangles) , hatches (600μm×600μm) and straight line trenches (100μm between each trench). The parameters for the laser processing were kept constant for all samples at 5W laser power and 1000mms^{-1} traverse speed, apart from the concentric circle pattern which was carried out with parameters of 70W laser power and 700mms^{-1} traverse speed. In addition, a non-irradiated sample was retained to be analysed and act as a reference.

Mechanical Roughening Procedure

For further verification of laser induced contact angle modification two samples were roughened manually using DA-F P220 emery paper. One sample was roughened using a zig-zag motion traversing from the top to the bottom of the sample (sample R1). The second sample (sample R2) was roughened by carrying out the same technique as the first sample, with the addition of rotating the sample through 90° and repeating the roughening method with the emery paper.

Topography, Wettability Characteristics and Surface Chemistry Analysis

After the patterning of the nylon 6,6 samples they were analysed using a number of techniques. Optical images of the irradiated samples were obtained using an optical microscope (Flash 200 SmartScope; OGP Ltd). The surface profiles were determined using a white light interferometer (WLI) (NewView 500; Zygo Ltd) with MetroPro and and TalyMap Gold Software. The Zygo WLI was setup using a ×10 Mirau lens with a zoom of ×0.5 and working distance of 7.6mm.

The samples were ultrasonically cleaned in isoproponal (Fisher Scientific, Ltd) for 3 minutes at room temperature before using a sessile drop device to determine various wettability characteristics, in accordance with the procedure detailed by Rance [20]. This was to allow for a relatively clean surface prior to any contact angle measurements being taken. The sessile drop device (OCA20; Dataphysics, Ltd) with SCA20 Software allowed the recent advancing and receding contact angles for triply distilled water and the recent advancing angle for diodomethane to be determined for each sample. By achieving the advancing and receding contact angles the hysteresis for the system was determined. In addition, by knowing the advancing contact angles for the two liquids it was possible to use the software to draw a Owens, Wendt, Rabel and Kaeble (OWRK) plot to determine the surface energy of the irradiated samples. For the two reference liquids the SCA20 software used the Ström et al. technique to calculate the surface energy of the material. It should be noted here that 10 contact angles in each instance were recorded to obtain a mean contact angle for each liquid. To avoid any possible experimental error as result of laser cutting the sample discs, all sessile drops where placed within a maximum 10mm radius of the centre of the sample discs.

Selected samples were analysed using X-ray photo-electron spectroscopy (XPS) and were also sputter coated with Au to attain adequate conductance and analysed using energy dispersive X-ray (EDX) analysis. This allowed any surface chemistry changes due to the laser irradiation to be quantified.

Results and Discussion

Analysis of Surface Topography Resulting from CO_2 Laser Irradiation

In order to achieve effective analysis of the laser irradiated samples an optical micrograph and WLI data was obtained for the non-irradiated reference sample. The micrograph of the reference sample, directly after CO_2 laser cutting, can be seen in Figure 1.

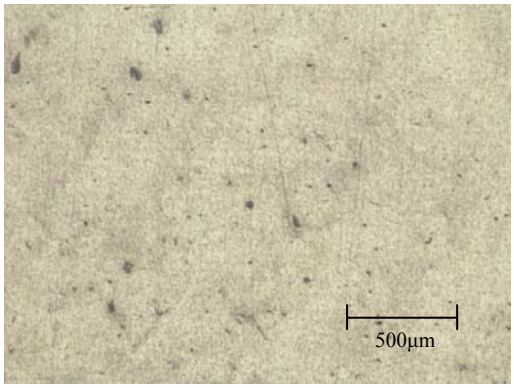

Figure 1 – Optical micrograph of the non-irradiated reference sample.

Figure 1 shows that there was debris that has arose from the CO_2 laser cutting, as indicated by the black spots on the image. The debris was removed during the ultrasonic cleaning process. The WLI continuous axonometric image (Figure 2) shows the reference sample after ultrasonic cleaing.

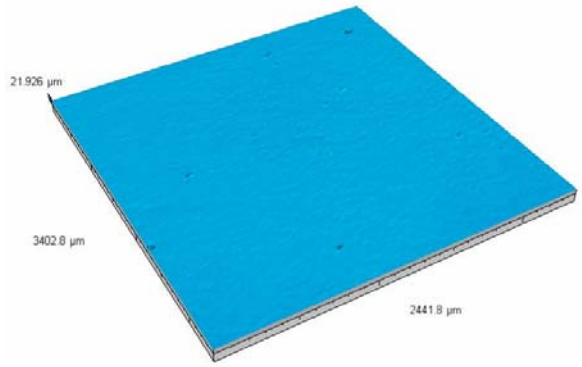

Figure 2 – Continuous axonometric image for the non-irradiated reference sample after ultrasonic cleaning.

The image obtained in Figure 2 allows one to see that the non-irradiated surface was relatively smooth in comparison to the irradiated samples and that most of the debris had been removed during the cleaning process. Further confirmation was determined by taking a profile extraction, as can be seen in Figure 3.

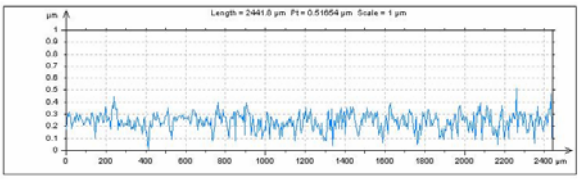

Figure 3 – Profile extraction of the reference sample surface shown in Figure 2.

Figure 3 confirms that the surface of the non-irradiated reference sample was relatively smooth, in comparison to the laser irradiated samples, with the highest peak on the surface being approximately 0.5µm, on average, however, the peaks reach approximately 0.3µm.

Because of the beam delivery mechanism of the Synrad CO_2 laser system, it was possible to generate a number of surface patterns on nylon 6,6 by scanning the CO_2 laser beam across the surface. Figure 4 shows an optical micrograph of straight line trenches generated into the nylon 6,6.

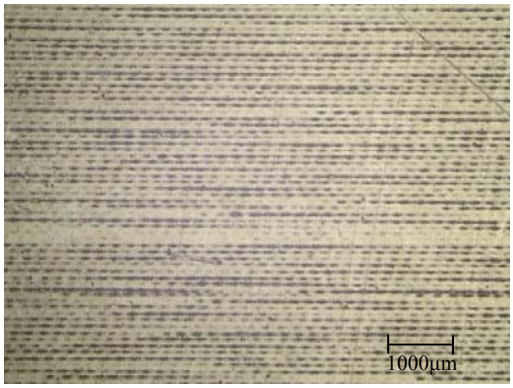

Figure 4 – Micrograph of straight line, parallel trenches.

From Figure 4 it is possible to see that the beam was scanned horizontally across the sample to produce the required pattern. As can be seen in Figure 4, the beam does not produce a solid continuous line. It is believed that this is due to the fact that the CO_2 laser melts the nylon 6,6 and as the beam moves away from that point, the melt resolidifies as a protrusion out from the surface. As a result, the melting and resolidifying of nylon 6,6 is evidently less predictable when compared to laser ablation [21]. The protrusions are more discernible from a WLI analysis, shown in Figure 5.

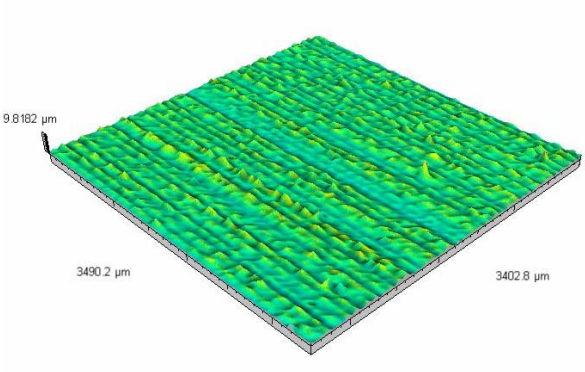

Figure 5 – Continuous axonometric image for the straight line, parallel trenches.

Figure 5 shows that the CO_2 laser gave rise to relatively good quality processing in terms of producing the straight line trenches. However, it can be seen from Figure 5 that there does appear to be slight differences in the heights of the peaks. In order to look at this into more depth a profile extraction graph was obtained perpendicular to the trenches, which can be seen in Figure 6.

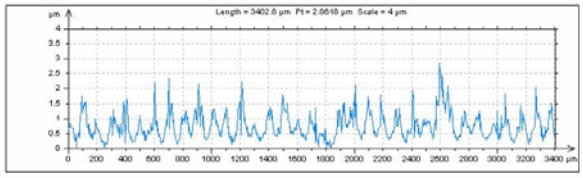

Figure 6 – Profile extraction of the surface shown Figure 5 perpendicular to the trenches.

The profile extraction graph, shown in Figure 6, indicates that there was some periodicity in the CO_2 laser generated trenches. It can also be seen in Figure 6 that the peaks are at differing values. This is believed to be due to the uncertainty in the melting and re-solidification.

The hatches pattern (Figure 7) shows the raised material to produce this topography.

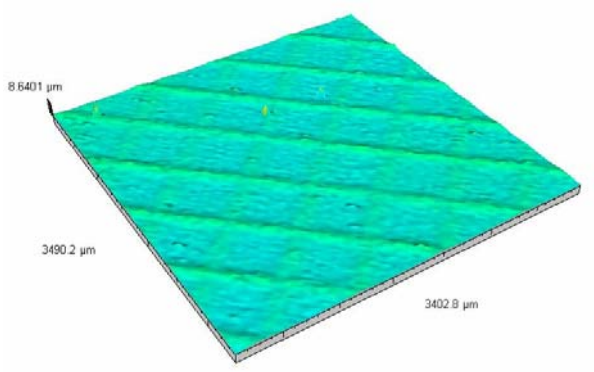

Figure 7 – Continuous axonometric image of the hatched generated surface pattern.

It would appear from Figure 7 that the hatch pattern has higher peaks in the horizontal axis (left to right) when compared to the vertical axis (top to bottom). In order to analyse this further a profile extraction was performed, given in Figure 8. The extraction was taken perpendicular to 4 protrusions on the horizontal axis (0 to 2500µm) and 4 protrusions on the vertical axis (2500 to 4500µm).

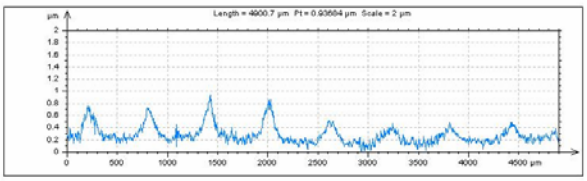

Figure 8 – Profile extraction of Figure 7 with the extraction been taken perpendicular to 4 protrusions on the horizontal axis and 4 protrusions on the vertical axis.

It is evident from Figure 8 that the largest peaks are on the horizontal axis (0 to 2500µm), with peak heights of 1µm. In contrast, the vertical axis (2500 to 4500µm) has peak heights of 0.5µm giving rise to a difference of about 0.5µm in height between the protrusions for both axis. This should not have occurred due to the fact that the same power and traverse speed was kept constant throughout the processing. However, due to limitations in the software it was possible that one axis could receive more than one scan across the material, when generating the pattern. This would mean that this axis would receive longer irradiation time in comparison to the other axis.

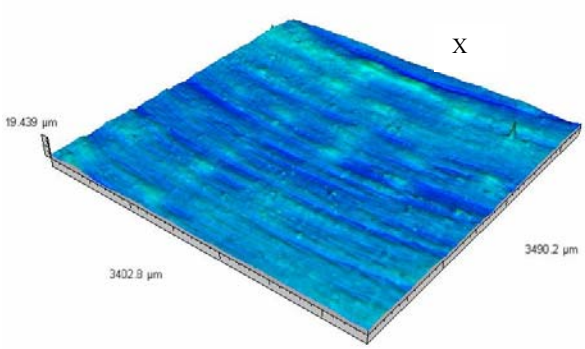

Figure 9 – Continuous axonometric image for a section of the generated spiral pattern.

The spiral pattern generated using the CO_2 laser system, which can be seen in Figure 9, shows the direction the way in which the beam was scanned across the surface, with the centre of the spiral being positioned to the top-right of the image (denoted as X in Figure 9). As the scanned lines of the spiral were too close together in comparison to the spot size, it should be noted here that the beam scan overlapped itself during the laser processing. This is confirmed by taking a profile extraction of the spiral pattern, Figure 10, shown in Figure 9.

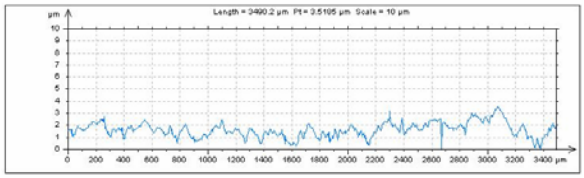

Figure 10 – Profile extraction of the spiral pattern shown in Figure 9.

A comparison of the surface data for the non-irradiated reference sample, given in Figure 3, with the profile extraction curve of the spiral pattern, shown in Figure 10, reveals that the spiral pattern brings about a rougher surface. This was a result of the spot size overlapping already irradiated areas, this in turn inherently removed the natural periodicity of the spiral pattern. Also, from Figure 10 the peak heights generated on account of CO_2 laser processing were of the order of 3µm

Following on from this it can be seen from Figure 11 that the centre of spiral was removed. This occurrence was caused by the spot size being larger than the initial outward movement from the centre of the spiral pattern, effectively resulting in a trepanning motion which drilled out the centre of the spiral.

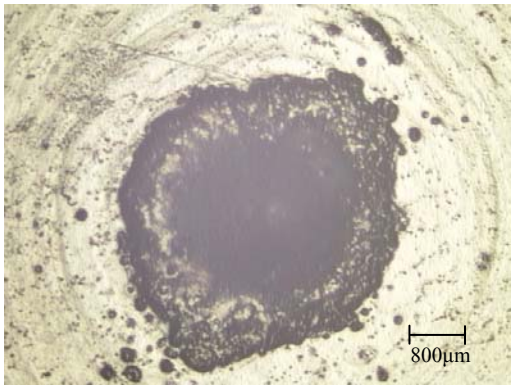

Figure 11 – Optical micrograph of the trepanned centre of the spiral pattern.

From Figure 11 one can see rupture sites where evolved gas bubbles, caused by excessive temperature rise resulting from beam overlap, have burst through the surface. This is also evident from Figure 14. In this instance the beam had passed over the corners more often than other sections of the triangular pattern, effectively causing the same excessive temperature rise that occurred for the spiral pattern.

Due to limitations of the CO_2 laser system the concentric circles sample had to be processed using a higher power of 7W and slower traverse speed of 700mms^{-1}. This also allows one to confirm that the scanned beam gave rise to a protrusion out of the surface as can be seen in Figure 12.

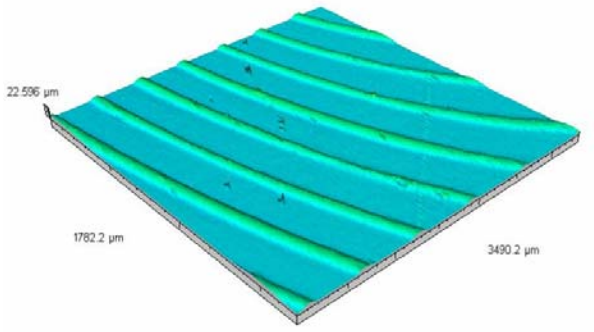

Figure 12 – Continuous axonometric for a section of the concentric circles sample.

In order to compare the surface shown in Figure 12 with the other surfaces a profile extraction graph, Figure 13, was drawn showing the profile perpendicular to the protrusions.

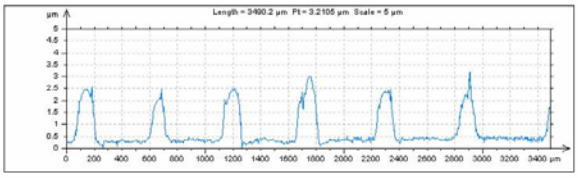

Figure 13 – Profile extraction graph for the surface shown in Figure 12 with the profile perpendicular to the protrusions being determined.

As can be seen in Figure 13, owing to the higher power and slower traverse speed, the protrusion of the pattern was considerably larger in comparison to the other samples that were irradiated using 5W and 1000mms^{-1}. This arises because more of the nylon 6,6 becomes molten and resolidifies.

The continuous axonometric image for the sample with a generated triangular pattern can be seen in Figure 14.

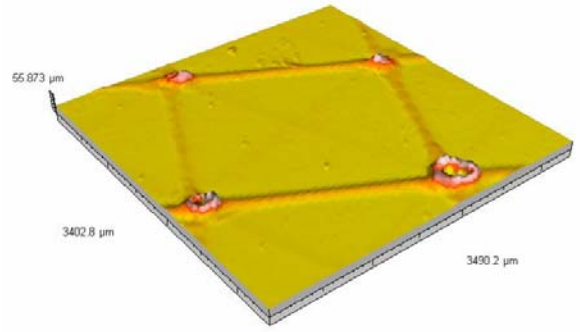

Figure 14 – Continuous axonometric image for a section of the triangular patterned sample.

From Figure 14 it can be seen that the triangular shapes were only slightly defined in the centre of the square. Also, because of the way in which the system scans the beam to produce the pattern, the protrusions at the corners of the square are considerably larger than the protrusion at the apex of the triangle (at the centre of the square pattern). This is due to the fact that the corners of the triangles that form the square receive more passes of the beam. As a result, the corners of the triangles that form the square pattern are melted and resolidified repeatedly, resulting in a crater where the sides protrude from the surface.

The mechanism active in creating the protrusions that form the patterns on the nylon 6,6 surface as a result of CO_2 laser irradiation were examined with WLI analysis. From Figures 7 to 14 it can be deduced that the mechanism for forming the protrusions was one in which the molten nylon 6,6 is forced up from the nominal surface. The upward force was likely to be generated by evolved gases and Marangoni flow [22].

More specifically, by taking into account $\frac{d\vartheta}{dT}$, with ϑ being the surface tension and T being the temperature, a flow shown in Figure 14 would occur if $\frac{d\vartheta}{dT} < 0$.

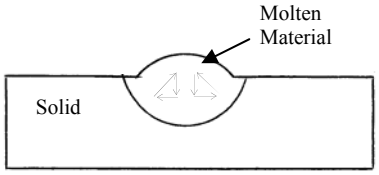

Figure 14 – Schematic diagram showing the flow arising for $\frac{d\vartheta}{dT} < 0$.

Figure 14 demonstrates that a rising flow within the molten material would make the centre of the material to rise up. By removing the heat quickly, as the laser beam scans away from the point, it can be seen that this will solidify allowing for the risen protruding shape to remain on the surface. Taking EDX and XPS analysis of a cross-section of the protrusions may identify any evolved gases that are trapped as a result of the laser-induced melting and resolidification.

Effects of Laser Irradiation on the Wettability Characteristics

As it has already been discussed, it is possible to see that the surface properties of a material has a major influence over the characteristic contact angle for that material. As such, the surface roughness parameters, contact angle and surface energy parameters were determined for each of the irradiated samples, including a non-irradiated reference sample to act as a reference. These results are given in Tables 1 and 2.

Table 1 – Results of the contact angle for triply distilled water and surface roughness for each sample.

Pattern Shape	Contact Angle (°)	Sa (µm)	Ra (µm)	Wa (µm)
Non-Irradiated	49.34	0.056	0.048	0.020
Straight Line Trenches	54.09	0.349	0.333	0.052
Hatch	50.37	0.136	0.085	0.055
Spiral	57.22	0.376	0.343	0.320
Concentric Circles	49.42	0.572	0.511	0.117
Triangles	49.98	0.523	0.803	1.737
R1	43.95	3.104	2.368	1.862
R2	38.37	3.735	3.055	3.568

The results given in Table 1 reveal that for all laser irradiated samples the surface roughness was increased sufficiently. In addition, it can be seen that the contact angle increased slightly for each of the laser irradiated samples in comparison to the non-irradiated reference sample. The spiral pattern gave the largest contact angle with 57.22° in contrast to the non-irradiated reference sample at 49.34°. It was also found that the hatch, concentric circles and triangular patterns produced contact angles that are similar to that obtained with the non-irradiated reference sample. This should not be the case as the roughness has been sufficiently amplified, especially in the cases of the concentric circles and triangular patterns each with Ra increases of 0.463 and 0.755µm, respectively. However, it should be noted that all of the three samples do possess large areas in which the surface is not modified and as a result, would have a large effect on the value of the contact angle. Also, depending on where the droplet was located on the surface would have a big influence on the contact angle determined.

The rise in contact angle shown in this study does not concur with current theory [12,13], which shows that the contact angle should decrease upon an increase of surface roughness. In order to explore this phenomenon surface energy component results were obtained for each sample. These can be seen in Table 2.

Table 2 – Results of the surface energy parameters for each of the samples.

Pattern Shape	Contact Angle (°)	Polar Component (mJm^{-2})	Dispersive Component (mJm^{-2})	Total Surface Energy (mJm^{-2})
Non-Irradiated	49.34	20.15	36.12	56.27
Straight Line Trenches	54.09	20.44	27.67	48.11
Hatch	50.37	28.60	24.59	53.19
Spiral	57.22	20.16	25.84	46.00
Concentric Circles	49.42	25.17	25.52	50.69
Triangles	49.98	24.17	26.44	50.61
R1	43.95	22.57	34.86	57.43
R2	38.37	24.68	36.85	61.53

Results stated in Table 2 show that for all samples the total surface energy decreased up to approximately $10mJm^{-2}$. However, the polar component, a factor that can give rise to a change in contact angle has increased for all samples. For instance, the greatest increase was given by the hatch pattern, with $8.45mJm^{-2}$ more than that of the non-irradiated reference sample. This also is not consistent with current theory as a rise in polar component should give rise to a reduction in contact angle as stated by Lawrence and Li [12].

Three samples: non-irradiated reference, spiral pattern and R1 were analysed using EDX and XPS analysis in order to determine any change in the surface O_2 content, as a result of the CO_2 laser irradiation. The results of the surface O_2 content can be seen in Table 3.

Table 3 – Surface O_2 Content for Selected Samples

Pattern Shape	Surface O_2 Content (%)	Contact Angle (°)
Non-Irradiated	19.58	49.34
Spiral	21.62	57.22
R1	20.21	43.95

The data given in Table 3 show that the surface O_2 content had increased for the spiral pattern after CO_2 laser processing by 2.04%. It is believed that this can be accounted to oxidation of the surface as the experiment was carried out in ambient air. This should give rise to a reduction in the contact angle; however, this is not being observed. The non-irradiated reference sample and R1 have equivalent surface O_2 content which signifies that the surface roughness of the R1 sample is the driver for the reduction in contact angle.

Determination of the Active Wetting Regime

The surface energy, XPS and EDX analysis for the CO_2 laser irradiated samples should produce samples which have a contact angle that is lower than that of the non-irradiated reference sample. To explore this phenomenon further, two samples were roughened using emery paper in the manner described above. The continuous axonometric images for these samples (R1 and R2) can be seen in Figure 15 and 16.

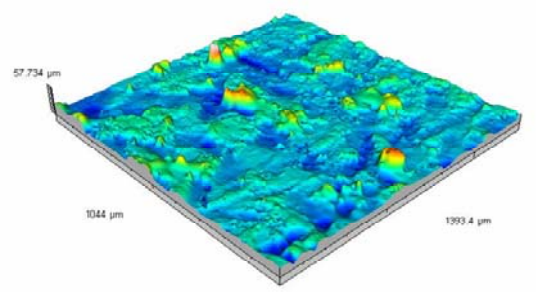

Figure 15 – Continuous axonometric image of the first emery paper roughened sample (Sample R1).

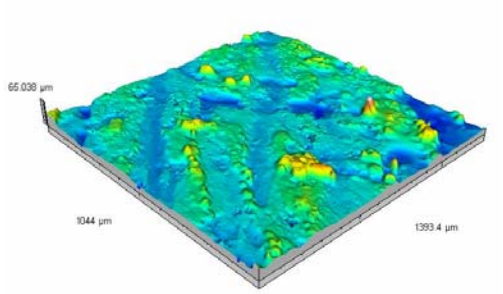

Figure 16 – Continuous axonometric image of the second emery paper roughened sample (Sample R2).

As a result of the mechanical roughening of the samples it can be seen from the results given in Tables 1 and 2 that an increase in the polar component and surface roughness has affected a significant reduction in contact angle, which concurs with Lawrence and Li [12]. Whereas the laser irradiated samples display more periodically patterned surfaces. The images shown in Figures 15 and 16 give no indication of a periodic pattern being induced on the surface of the nylon 6,6 samples. This is significant as these laser-induced periodic patterns appear to have an extremely large effect on the wettability characteristics of the samples; namely the contact angle. As discussed by Jung and Bhushan [23], there are two regimes in which a material can wet: the Cassie-Baxter and Wenzel regimes. In the case of the Wenzel regime, shown schematically in Figure 17, the whole sample surface is wetted such that the droplet is in complete contact with the entire contact surface area.

Figure 17 – Schematic diagram showing a droplet of water on a patterned surface giving rise to the Wenzel wetting regime.

On the other hand, the Cassie-Baxter regime, shown schematically in Figure 18, allows the droplet to rest upon the roughened surface peaks only, resulting in the formation of air gaps between the droplet and the surface at the base of the peaks.

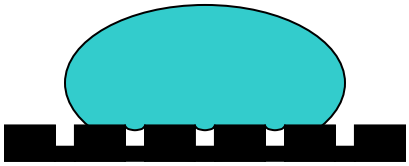

Figure 18 – Schematic diagram showing a droplet of water on a patterned surface giving rise to the Cassie-Baxter wetting regime.

It is proposed here that a change from the Wenzel wetting regime to the Cassie-Baxter wetting regime, could be the reason due to the increased contact angle observed for the CO_2 laser irradiated samples, since the Cassie-Baxter regime gives rise to larger contact angles in comparison with the Wenzel regime. It is therefore proposed that the form and dimensions of the laser-induced surface patterns is the main driver for the manipulation of the wettability characteristics. This implies that the roughness (Table 1), surface energy components (Table 2) and surface O_2 content (Table 3) do not play the governing role observed by other workers when conducting laser treatment of polymers without patterning [12].

Conclusions

Throughout this study it has been observed that it is possible to generate various surface patterns using the Synrad CO_2 laser marking system. The process in which the nylon 6,6 samples were patterned with the laser were found to be due to a thermolytical mechanism, in which the surface is melted and resolidified. In addition, it was found that due to this mechanism, oxidation took place allowing a rise in surface O_2 content to be achievable. As a result, it can be seen that additional research into laser processing in various ambient gases may provide one with a way to efficiently modify the surface chemical composition.

The wettability characteristics, in this research, does not concur with current theory as all obtained parameters (roughness, surface O_2 content and surface energy components) imply that the contact angle of the laser irradiated samples should have decreased in comparison to the non-irradiated reference sample. However, this is not the case and the contact angle has been shown to increase following CO_2 laser induced patterning. It has been proposed that the explanation for this phenomenon could be due to a change in wetting regime from Wenzel to the Cassie-Baxter regime. If this was the case then it would be possible to elucidate as to why an increase in contact is occurring. In order to validate this, more research is required to ascertain the type of wetting that is occurring.

Acknowledgements

We would like to thank Matthew Gibson, Peter Wileman and David Britton for all of their much appreciated support. This study is financially supported by the EPSRC (No. EP/E046851/1).

References

1. Mao, C. et al. (2005) In vitro studies of platelet adhesion on UV radiation-treated nylon surface. Carbohydrate Polymers, 59, 19-25.

2. Karaca, E. et al. (2008) Analysis of the Fracture Morphology of Polyamide, Polyester, Polypropylene, and Silk Sutures Before and After Implantation In Vivo. Journal of Biomedical Materials Research Part B: Applied Biomaterials.

3. Makropoulou, M. et al. (1995) Ultra-violet and Infra-red Laser Ablation Studies of Biocompatible Polymers. Lasers in Medical Science, 10, 201-206.

4. Benson, R. S. (2002) Use of Radiation in Biomaterials Science. Nuclear Instruments and Methods in Physics Research B, 191, 752-757.

5. Arefi-Khonsari, F. et al. (2005) Processing of Polymers by Plasma Technologies. Surface and Coatings Technology, 200, 14-20.

6. Pappas, D. et al. (2006) Surface Modification of Polyamide Fibers and Films using Atmospheric Plasmas. Surface and Coatings Technology, 201, 4384-4388.

7. Harnett, E. M. et al. The surface energy of various biomaterials coated with adhesion molecules used in cell culture. Colloids and Surfaces B: Biointerfaces, 55, 90-97.

8. Yu, F. et al. (2005) Laser interference lithography as a new and efficient technique for micropatterning of biopolymer surface. Biomaterials, 26, 2307-2312.

9. Mirzadeh, H. et al. (2003) Influence of laser surface modifying of polyethylene terephthalate on fibroblast cell adhesion. Radiation Physics and Chemistry, 67, 381-385.

10. Pfleging, W.. et al. (2007) Laser-Assisted Modification of Polystyrene Surfaces for Cell Culture Applications. Applied Surface Science, 253, 9177-9184.

11. Ratner, B. D. et al. (2004) Biomaterials Science. Second ed. San Diego, California, USA: Elsevier Academic Press.

12. Lawrence, J. et al. (2001) Modification of the Wettability Characteristics of Polymethyl Methacrylate (PMMA) by Means of CO_2, Nd:YAG, Excimer and High Power Diode Laser Irradiation. Materials Science and Engineering A, 303, 142-149.

13. Hao, L. et al. (2005) Laser surface treatment of bio-implant materials. New Jersey, USA: John Wiley & Sons Inc.

14. Lai, J. et al. (2006) Study on Hydrophilicity of Polymer Surfaces Improved by Plasma Treatment. Applied Surface Science, 252, 3375-3379.

15. Ma, Z. et al. (2007) Surface modification and property analysis of biomedical polymers used for tissue engineering. Colloids and Surfaces B: Biointerfaces, 60, 137-157.

16. Mirzadeh, H. et al. (1995) Cell attachment to laser-induced AAm-and HEMA-grafted ethylene-propylene rubber as biomaterial: *in vivo* study. Biomaterials, 16, 641-648.

17. Kim, M. S. et al. (2007) Gradient polymer surfaces for biomedical applications. Progress in Polymer Science.

18. Ball, M. D. et al. (2004) Cell interactions with laser-modified polymer surfaces. Journal of Materials Science: Materials in Medicine, 15, 447-449.

19. Silfvast, W. T. (1996) Laser fundamentals. Cambridge, UK: Cambridge University Press.

20. Rance, D. G. (1982) Chapter 6 - thermodynamics of wetting: From its molecular basis to technological application. In: Brewis DM, editor. Surface Analysis and Pretreatment of Plastics and MetalsEssex, UK: Applied Science Publishers, 1982. p. 121.

21. Waugh, D. G. et al. (2008) A comparative study into varying the factors influencing the biocompatibility of a polymeric biomaterial using CO_2 and F_2 lasers. Submitted to Optics and Lasers in Engineering.

22. Bauerle, D. (2000) Laser processing and chemistry. Third ed. New York, USA: Springer-Verlag, p177-179.

23. Jung, Y. C. et al. (2007) Wetting transition of water droplets on superhydrophobic patterned surfaces. Scripta Materialia, 57, 1057-1060.

Meet The Author

David Waugh is currently undertaking a Ph.D at the Wolfson School of Mechanical and Manufacturing Engineering, Loughborough University, UK under the supervision of Dr. Jonathan Lawrence. His research is focusing on using laser surface treatment of polymeric biomaterials for enhanced cell response. He obtained his MPhys Hons. in Physics with Lasers and Photonics and MSc in Laser Applications in Micro-Machining and Processing from the University of Hull, UK.